

Back Side Ablation of SiC Diodes using a q-switched NIR Laser

B. Adelman*, A. Hürner**, G. L. Roth*, R. Hellmann*

*University of Applied Sciences Aschaffenburg, Würzburger Str. 45, 64743 Aschaffenburg, Germany
E-mail: Benedikt.adelmann@h-ab.de

**Chair of Electron Devices, University of Erlangen-Nuremberg, Schottkystrasse 10, 91058 Erlangen, Germany

We study pulsed fiber laser back side ablation of silicon carbide diodes. With the objective to thin the SiC substrate thickness without damaging the semiconductor device or altering its electrical characteristics, we investigate the ablation characteristics of silicon carbide and determine the ablation threshold, rate and quality as well as the material composition at the ablated surface. Based on optimized process parameters, including track distance, laser repetition rate and scanning velocity, we micro structure the substrate of SiC diodes and compare its electrical characteristic to an unprocessed device. Our results prove that the typical diode characteristic and built-in voltage are not affected by the laser ablation process. Fiber laser back side ablation therefore offers a precise and efficient micro structuring approach for substrate thinning in silicon carbide technology.

DOI: 10.2961/jlmn.2015.02.0016

Keywords: Laser ablation, fiber laser, SiC diode, serial resistance

1. Introduction

Silicon substrates form the fundamental basis of most semiconductor devices with all relevant technological process steps being well established. However, for new applications in high power electronics as well as for ultrafast electronic devices silicon has physical limitations. In contrast, silicon carbide (SiC) has distinct advantages over silicon. The most important advantages of SiC are i) the higher band gap of 3.2 eV in 4H-SiC, ii) the thermal conductivity being twice as high as in silicon, iii) a ten times higher electrical disruptive strength and iv) the higher saturated electron drift velocity, which is twice as high as in silicon [1] [2].

In non-power electronic devices based on silicon substrates all electric contacts are, in general, located on the top side of the devices and the electrical current flows exclusively between these contacts within thin layers beneath the surface. Except from these thin layers on the top side, the volume of the substrate itself does not contribute to the electrical conduction. Opposite to this, in power electronics based on silicon as well as in silicon carbide based devices the electrical current flows from the top side to the bottom which necessitates electrical front- and backside contacts [3]. This architecture has the disadvantage of a long conducting path in the bulk material which results in an additional serial resistance. As the serial resistance increases with the substrate thickness, it is therefore highly desirable to reduce the substrate thickness.

However, due to the high chemical inertness of SiC, common semiconductor micromachining techniques such as, e.g., etching with potassium hydroxide or ethylenediamine are inapplicable [4]. Possible wet etching methods for SiC require elevated temperatures as, e.g. phosphoric acid at 215 °C or alkaline solutions of $K_3Fe(CN)_6$ at temperatures of higher than 100 °C [5]. As these conditions are unfavorable, the standard method for SiC micromachining is dry etching [6] [7]. The most common dry etching methods are SF_6 with O_2 , CF_4 optionally with O_2 , Cl_2/Ar or Ar . The achieved etching rates are between 27 nm/min and

970 nm/min [8] [9] [10]. Further etching methods are electrochemical etching [11] [12] and photo-electrochemical etching [13], which can achieve higher etching rates of 2 $\mu\text{m}/\text{min}$.

Yet, these etching methods are disadvantageous as they require reticles and etch stops [4]. Especially for 3 dimensional structures requiring several etching steps, multiple reticles are needed. This, however, significantly increases processing costs. In contrast to etching, laser micro processing obviates any chemistry and offers a high degree of geometrical freedom without requiring mask techniques.

Laser ablation and drilling of SiC has been demonstrated using short and ultrashort pulsed lasers with pulse lengths in the nanosecond to femtosecond regime. Reitano et al. report an ablation threshold of 2 J/cm^2 for 6H-SiC using a nanosecond XeCl excimer at 288 nm [14]. Between 3 J/cm^2 and 9 J/cm^2 an ablation of 55 nm per pulse was found. Gupta et al. also report the ablation threshold of 2 J/cm^2 employing a 248 nm KrF Excimer laser [15]. Maximum ablation rates of 105 nm per pulse are found at 15 J/cm^2 . In a comparative study it was shown that the ablation rate of 6H-SiC is about 5 nm per pulse higher as compared to 4H-SiC.

In contrast to excimer lasers with high pulse energies in the range between 10 mJ and 300 mJ at low pulse repetition rates in the range of 10 Hz to 300 Hz, frequency tripled Nd:YAG lasers provide higher repetition rates with lower pulse energies. Krueger et al. [16] [17] used a frequency tripled Nd:YAG laser at 355 nm with 73 J/cm^2 fluence (65 μJ on 15 μm diameter) and a repetition rate of 10 kHz to ablate blind vias in SiC. For 380 μm deep holes with 75 μm diameter 2 seconds are required. To form a flat bottom of the blind holes, after the laser process IPC etching was applied.

To reduce the thermal energy deposited into the material Molian et al. used a 2 ps ultrashort pulsed laser with 1552 nm wavelength and 5 μJ pulse energy to ablate 4H-SiC [18]. Using such ultrashort pulsed laser, it was possible to ablate a 26 μm deep cavity with sharp edges, no cracks

and no melt formation. The maximum ablation rate is determined to be 18 nm per pulse at 10 J/cm². For using a 1028 nm Ti-Sapphire laser with a pulse duration of 200 fs, Farsari et al. calculated the dimension of the laser induced heat affected zone in SiC to 3.6 μm [19] [20].

Though it has been demonstrated that laser ablation of SiC semiconductors is possible with UV and ultrashort pulsed lasers, as summarized above, the influence of such ablation processes on the function of semiconductor devices is so far not addressed in literature. Taken into account the device architecture, which encompasses the device beneath the front side contact on the underlying substrate (cf. figure 1), it has to be considered that during substrate ablation from the back side laser radiation will also penetrate the device region. The amount of laser energy reaching the electrical device depends on the absorption which in turn depends on laser wavelength. As a matter of course, any adverse effects or damage of the device during laser ablation has to be avoided. In this contribution we therefore investigate the influence of back side substrate ablation on the function of a SiC diode.

2. Experimental

2.1 SiC Diodes

The schematic cross section of the SiC diode chosen for the experimental study of laser ablation is depicted in figure 1. The diode is grown on a 5×10^{18} 1/cm³ n-doped 4-H silicon carbide substrate with a thickness of 400 μm, on which a typical backside metallization stack is deposited. On the front side, a 10 μm epitaxial layer of p-doped SiC with an acceptor concentration of approximately 10^{15} 1/cm³ is grown, forming the diode. An additional 800 nm deep p-doped zone with a carrier concentration of 10^{19} 1/cm³ is implanted into the front side p-SiC epitaxial layer to achieve an electrical contact to the metal layer above. The electrical front contact is subsequently completed by a 100 nm thin titanium layer followed by a 4 μm thick aluminum layer.

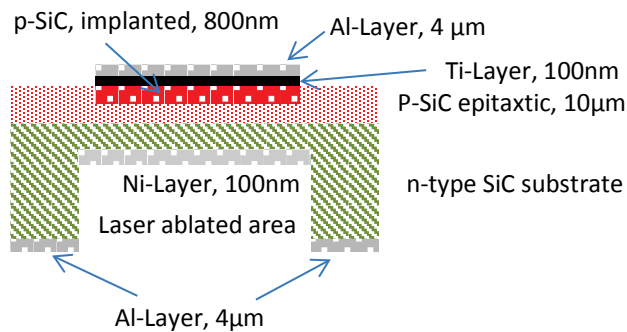


Figure 1: Architecture of the laser processed SiC diode

Laser ablation is carried out from the back side to reduce the thickness of the SiC n-type substrate. After ablation a 100 nm thin nickel layer is sputtered on the ablated area to renew the electrical back side contact and to facilitate electrical measurements of the diode characteristics.

At the laser wavelength employed in this study (1070 nm), we determined the optical transmission of the substrate to 44 % and the reflection to 32 %. The resulting absorption of 24 % corresponds to an absorption coefficient of 1062 m⁻¹ and a penetration depth of 940 μm. Please note that these measurements were conducted at room temperature. These optical properties, however, may significantly alter at high temperatures which occur during laser processing. Nonetheless, the high transmission indicates the possibility to affect the active device on the front side during laser ablation.

2.2 Laser system

For the experiments a pulsed (Q-switched) 20 W fiber laser is used (YLP Series, IPG Photonics). The laser is specified by an emission wavelength of 1070 nm, a pulse length of 100 ns, and a beam quality of $M^2 = 1.6$. The repetition rate can be adjusted between 2 kHz and 80 kHz with the average power of 20 W being available at 20 kHz. The maximum pulse energy is 1 mJ and the maximum fluence is 128 J/cm² for a 45 μm spot diameter. At repetition rates below 20 kHz the average power decreases at constant pulse energy. Above 20 kHz the average power remains constant with a decreasing the pulse energy. The output power can get adjusted between 10 % and 100 % of the nominal power of 20 W.

The laser beam is positioned by a galvanometer (Raylase SuperScan) with 163 mm focal length. This scanner has a maximum positioning speed of > 7 m/s deflected over a range of 110x110 mm².

3. Results and Discussion

3.1 Laser ablation characteristics of SiC

To facilitate a controlled back side laser ablation of the SiC substrate, fundamental ablation characteristics, such as ablation threshold, rate and quality as well as the material composition at the ablated surface, have to be initially determined. For the material under study, we have measured an ablation threshold of 30 J/cm² for 100 pulses according to the most commonly used procedure by Liu et al. [21]. This is considerable higher as compared to thresholds reported for ablation using UV excimer or picosecond lasers [14] [15] [18], which is attributed to the lower IR absorption of the fiber laser and its longer pulse length. Nevertheless, the concession of a higher ablation threshold is associated with a significantly simpler and cost efficient fiber laser system.

To reduce the SiC substrate thickness, a larger area with defined depth has to be ablated in a multi pass, meander type scan. To optimize such a scan strategy, we have investigated the influence of track distance, pulse repetition rate, and scan velocity (both define the pulse overlap) on the ablation rate, surface roughness, edge steepness and chipping of the semiconductor material. Since this contribution focusses on the function of the SiC diode after back side laser ablation, here we only briefly summarize the results of this optimization. As a consequence, the track distance of the meander type scan path is chosen to 36 μm (laser spot diameter is 45 μm). A lower track distance leads to a higher surface roughness and a higher track distance results in an incomplete ablation. The pulse repetition rate is set to

2 kHz (minimum of the laser system) with higher repetition rates resulting in a higher roughness and lower edge steepness. Finally, a scanning velocity of 20 mm/s is used as higher velocities lead to chipping of the material next to the ablated area. In turn, lower scanning velocities result in a higher surface roughness of the ablated area. Employing this parameter combination (track distance 36 μm , 2 kHz repetition rate and 20 mm/s) as a trade of between low surface roughness, avoidance of chipping and high process speed, the ablation rate is determined to 0.58 mm^3/min , which is notably higher as compared to the rate of 0.0018 mm^3/min reported for a frequency tripled Nd:YAG laser by Kreutz et al. [22].

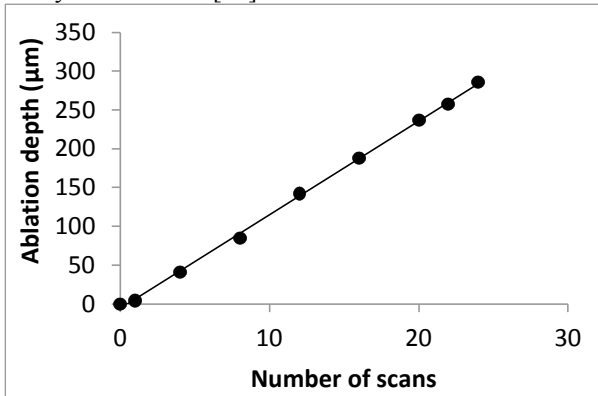


Figure 2: Ablation depth as a function of the number of scans (repetition rate 2 kHz and scanning speed 20 mm/s)

To achieve a defined ablation depth, multiple scans are necessary. Figure 2 shows the ablation depth as a function of the number of scans. Apparently, the ablation depth increases linearly with the number of scans with 12 μm per scan. This linear dependence allows to easily control the ablation depth by adjusting the number of scans. To evaluate the accuracy of this multi pass ablation process we processed multiple specimens and determined the standard error of the achieved ablation depth. We found standard errors of 0.8 μm (0.7%) for an ablation depth of 110 μm and 1.2 μm (0.4%) for 310 μm ablation depth, highlighting the high accuracy of the process.

With respect to any subsequent processing of the semiconductor device, e.g. metal deposition or etching, the surface roughness after laser ablation is of importance. We therefore have measured the surface roughness (Ra) of the ablated area using a laser scanning microscope. Figure 3 depicts the roughness as a function of the ablation depth. Starting from $Ra = 1 \mu\text{m}$ for the untreated surface, laser ablation roughens the surface with Ra depending linearly on the ablation depth. Please note that for these experiments the optimized laser parameters described above have been used (track distance 36 μm , pulse repetition rate 2 kHz and scan speed 20 mm/s).

Besides the surface roughness, for subsequent processes the material composition on the ablated surface is also of importance, e.g. for electrical contact generation by metalization [23]. We, therefore, have determined the composition by means of an EDX analysis prior and after laser ablation.

In course of the laser ablation, a white powder is observable on the treated surface, which is easily removable in an ultrasonic bath. This is identified as SiO_2 , with the EDX analysis determining oxygen in the range of 23 at%. This white powder was also reported by Kreutz et al. [22] with an oxygen content of 18 at%.

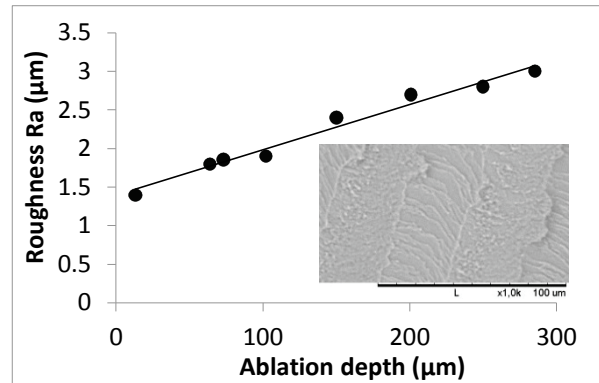


Figure 3: Surface roughness (Ra) as a function of the ablation depth. The inset depicts a SEM image of the laser ablated area, in which the adjacent ablation tracks can be seen.

After back side ablation of 100 μm (i.e. the 4 μm aluminum layer and 96 μm SiC are removed, cf. figure 1) and ultrasonic cleaning we find that the composition of the SiC substrate on the surface is altered. In particular, the amount of silicon is reduced as compared to untreated regions by a few percent, while the amount of carbon is correspondingly increased and an additional 2 at% aluminum is found. We attribute both the reduced silicon and increased carbon portion to the laser induced ejection of liquid silicon. According to Samant et al. [24], the latter is formed by a decomposition of SiC into solid carbon and liquid silicon at elevated temperatures during the ablation process. As the silicon is ejected, the proportional composition at the surface is shifted in favor of carbon.

3.2 Electrical characteristics of back side ablated SiC diodes

Based on these laser ablation characteristics, SiC diodes are back side ablated to reduce the thickness of the SiC substrate. To verify that after laser ablation the function of the semiconductor diode is not negatively affected, we structured 2x2 mm^2 wells with different depths (200 μm , 301 μm , and 329 μm) into the substrate. According to figure 2, the ablation depth is controlled by the number of meander type scans with the process parameters being track spacing of 36 μm , pulse repetition rate 2 kHz, and scanning speed 20 mm/s, respectively. As for the meander type scan the edges of the well experience a longer laser exposure during the inversion of the scanning direction, an additional deepening in excess of the ablated layer is observed. In this respect, it is worthwhile to mention that for a well of 329 μm depths only a thin substrate layer of about 70 μm remains, which is associated by the risk of mechanical breakup. In case of the 329 μm well, we therefore cascaded the well structure by two additional steps. Figure 4 shows this cascaded well structure as measured by a laser scan-

ning microscope, revealing the high quality and accuracy of the laser micro structuring process. Table 1 summarizes the processing time and measured roughness of the three wells generated in SiC.

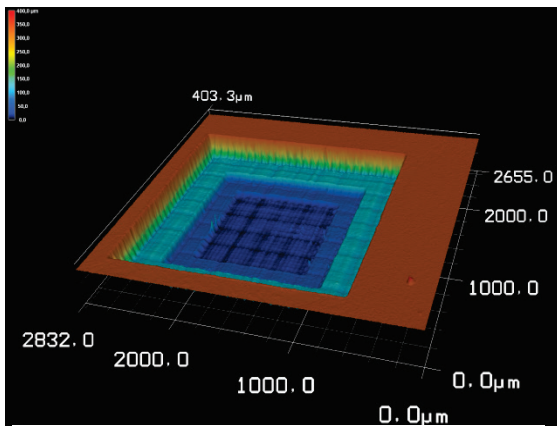


Figure 4: Laser scanning image of a 329 μm deep groove with 3 cascaded steps

After back side laser ablation the diodes are cleaned for 5 minutes in an ultrasonic bath to remove any debris. Afterwards a 100 nm nickel layer is sputtered onto the ablated area to form the new back side electrical contact. The electrical characteristics of the diode are determined by measuring the diode current as a function of voltage. Figure 5 compares this diode characteristic for an unprocessed reference device and the laser processed specimen. The reference diode is characterized by a reverse current of 0.1 μA at 5 V and a built-in voltage of 2.5 V.

Table 1: Depth, roughness and processing time of back side ablated SiC diodes

Depth (μm)	Roughness Ra (μm)	Processing Time (s)
200 (±0.8)	3.3	124.2
301 (±1)	3.4	151.4
329	3.8	158.3

The results depicted in figure 5 highlight that the typical diode characteristic of an exponential dependence between diode current and applied voltage is not affected by the laser ablation process, i.e. the semiconductor diode is neither damaged nor negatively influenced. In addition, the built-in voltage remains unchanged at 2.5 V and in reverse direction of up to -5 V no significant change is ascertained (the reverse current at 5 V is slightly reduced on the order of 0.06 μA, which is not resolved on the current scale in the figure 5).

For voltages above the built-in voltage the diode current is considerably reduced as compared to the reference diode, indicating an increasing forward voltage. However, as the experimental results in figure 5 show, this reduction does not unambiguously scale with the ablation depth. Hence, we conclude that the contact resistance between SiC and nickel dominates the measured resistance rather than the path resistance of the remaining SiC substrate. The contact resistance can be estimated by the additional voltage drop of a processed diode as compared to the reference

diode at constant current. For instance, at a current of 100 mA in the reference specimen a voltage drop of 3 V is observed and for the 200 μm ablated sample the voltage drop is measured to about 5 V (cf. figure 5). From this voltage difference of 2 V at 100 mA which drops at the back side contact the contact resistance is estimated to be

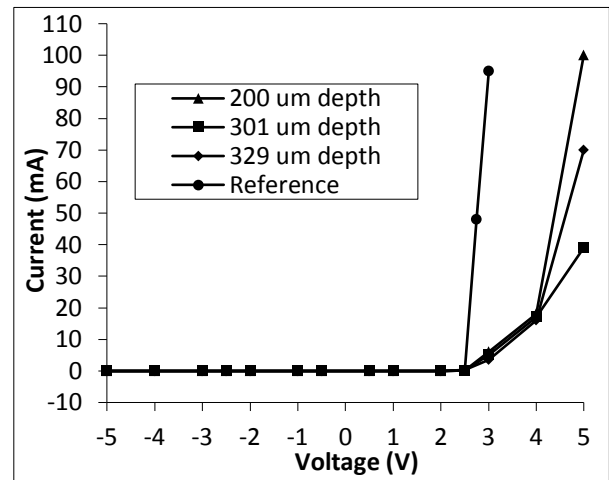


Figure 5: Current over voltage characteristic of the reference diode and the laser structured diodes.

about 20 Ω which is not unusual for a barely optimized metal SiC contact [23]. Nonetheless, these results clearly demonstrate that laser ablation can be employed to structure SiC diodes under perpetuation of the device characteristics. This in turn offers an innovative approach to thin SiC devices.

4. Conclusion

We have demonstrated that laser ablation using pulsed fiber laser can be employed to thin silicon carbide substrates beneath a functional diode without damaging the semiconductor device or altering its electrical characteristics. Especially, the built-in voltage and the typical current-voltage characteristics are unaffected by the laser process.

To enable high quality back side laser ablation of the SiC substrates, the ablation characteristics, such as ablation threshold, ablation rate and surface quality have been determined to identify an optimized parameter range for the ablation. In particular, the ablation rate is found to be 0.58 mm³/min allowing an efficient, high quality and precise ablation process.

References

- [1] T. Mnatsakanov, L. Pomortseva and S. Yurkov, "Semiempirical model of carrier mobility in silicon carbide for analyzing its dependence on temperature and doping level," *Physics and Astronomy*, pp. 394-397, 4 35 2001.
- [2] M. Ostling, "High power devices in wide bandgap semiconductors," *Science China*, p. 1087-1093, 5 2011.
- [3] T. Chow, N. Ramungul, J. Fedison and Y. Tang, "SiC Power Bipolar Transistors and Thyristors," in *Silicon Carbide*, Berlin, Springer, 2003, pp. 737-764.

- [4] C. A. Zormann and M. Mehregany, "Micromachining of SiC," in *Silicon Carbide*, Berlin, Springer, 2004, pp. 671-698.
- [5] D. Zhuang and J. J. Edgar, "Wet etching of GaN, AlN, and SiC: a review," *Materials Science and Engineering*, pp. 1-46, 48 R 2005.
- [6] H. Cho, P. Leerunyawarat, D. C. Hays, S. Pearton, S. Chu, R. Strong, C. Zetterling, M. Ostling and F. Ren, "Ultradeep, low-damage dry etching of SiC," *Applied Physics Letters*, pp. 739-741, 6 76 2000.
- [7] L. Jiang, R. Cheung, M. Hassan, A. Harris, J. Burdess, C. Zorman and M. Mehregany, "Fabrication of SiC microelectromechanical systems using one-step dry etching," *Journal of Vacuum Science & Technology B*, pp. 2998-3001, 6 21 2003.
- [8] J. Sugiura, W. Lu, K. Cadien and A. Steckl, "Reactive ion etching of SiC thin films using fluorinated gases," *Journal of Vacuum Science & Technology B*, pp. 349-354, 1 4 1986.
- [9] L. Jiang, N. Plank, M. Blauw, R. Cheung and E. Drift, "Dry etching of SiC in inductively coupled Cl₂/Ar plasma," *Journal of Physics D: Applied Physics*, p. 1809, 13 37 2004.
- [10] F. Khan and I. Adesida, "High rate etching of SiC using inductively coupled plasma reactive ion etching in SF₆-based gas mixtures," *Applied physics letters*, pp. 2268-2270, 15 75 1999.
- [11] V. Petrova-Koch, O. Sreseli, G. Polisski, D. Kovalev, T. Mischik and F. Koch, "Luminescence enhancement by electrochemical etching of SiC (6H)," *Thin Solid Films*, pp. 107-110, 1 255 1995.
- [12] S. Rysy, H. Sadovskii and R. Helbig, "Electrochemical etching of silicon carbide," *Journal of Solid State Electrochemistry*, pp. 437-445, 7-8 3 1999.
- [13] J. Shor and A. Kurtz, "Photoelectrochemical Etching of 6 H-SiC," *Journal of the Electrochemical Society*, pp. 778-781, 3 141 1994.
- [14] R. Reitano, P. Baeri and N. Marino, "Excimer laser induced thermal evaporation and ablation of silicon carbide," *Applied surface science*, pp. 302-308, 96 1996.
- [15] S. Gupta, B. Pecholt and P. Molian, "Excimer laser ablation of single crystal 4H-SiC and 6H-SiC wafers," *Journal of Materials Science*, pp. 196-206, 46 2011.
- [16] O. Krueger, G. Schoene, T. Wernicke, W. John, J. Wurfl and G. Traenkle, "UV laser drilling of SiC for semiconductor device fabrication," *Journal of Physics*, pp. 740-744, 59 2007.
- [17] O. Krueger and R. Grundmueller, "UV Laser Processing for Semiconductor Devices," *Laser Technik Journal*, pp. 26-30, 10 2013.
- [18] P. Molian, B. Pecholt and S. Gupta, "Picosecond pulsed laser ablation and micromachining of 4H-SiC wafers," *Applied Surface Science*, pp. 4515-4520, 255 2009.
- [19] M. Farsari, G. Filippidis, S. Zoppel, G. Reider and C. Fotakis, "Efficient Femtosecond laser micromachining of bulk 3C-SiC," *Journal of Micromechanics and Microengineering*, pp. 1786-1789, 15 2005.
- [20] M. Farsari, G. Filippidis, S. Zoppel, G. Reider and C. Fotakis, "Micromachining of Silicon Carbide using femtosecond lasers," *Journal of Physics: Conference Series*, p. 84-87, 59 2007.
- [21] J. M. Liu, "Simple technique for measurements of pulsed Gaussian-beam spot sizes," *Optics Letters*, vol. 7, no. 5, pp. 196-198, May 1982.
- [22] E. Kreutz, R. Weichenhain, A. Horn and R. Poprawe, "Manufacturing of Precise SiC Components by Nd: YAG Laser Radiation," *Solid State Phenomena*, pp. 441-446, 80 2001.
- [23] B. Adelman, A. Hürner, T. Schlegel, A. J. Bauer, L. Frey and R. Hellmann, "Laser Alloying Nickel on 4H-Silicon Carbide Substrate to Generate Ohmic Contacts," *Journal of Laser Micro/Nanoengineering*, Vols. 8-1, pp. 97-101, 2013.
- [24] A. Samant, C. Daniel, R. Chand, C. Blue and N. Dahotre, "Computational approach to photonic drilling of advanced carbide," *The International Journal of Advanced Manufacturing Technology*, pp. 704-713, 45 2009.
- [25] S. Baudach, J. Bonse and W. Kautek, "Ablation experiments on polyimide with femtosecond laser pulses," *Applied Physics A*, pp. 395-398, 69 1999.
- [26] J. Bonse, J. Wrobel, J. Krueger and W. Kautek, "Ultrashort-pulse laser ablation of indium phosphide in air," *Applied Physics A*, pp. 89-94, 72 2001.
- [27] W. Shi, Y. Zheng, H. Peng, N. Wang, C. Lee and S. Lee, "Laser ablation synthesis and optical characterization of silicon carbide nanowires," *Journal of the American Ceramic Society*, pp. 3228-3230, 83 2000.
- [28] U. Engelhardt, J. Hildenhagen and K. Dickmann, "Micromachining using high-power picosecond lasers," *Laser Technik Journal*, vol. 8, no. 5, pp. 32-35, 2011.

(Received: October 31, 2015, Accepted: March 22, 2015)